Silver nanoparticles loaded on Cu-doped TiO_2 for the effective reduction of nitro-aromatic contaminants

Agileo Hernández-Gordillo, Vicente Rodríguez González

PII: S1385-8947(14)00825-0
DOI: http://dx.doi.org/10.1016/j.cej.2014.05.148
Reference: CEJ 12322

To appear in: *Chemical Engineering Journal*

Please cite this article as: A. Hernández-Gordillo, V.R. González, Silver nanoparticles loaded on Cu-doped TiO_2 for the effective reduction of nitro-aromatic contaminants, *Chemical Engineering Journal* (2014), doi: http://dx.doi.org/10.1016/j.cej.2014.05.148

Silver nanoparticles loaded on Cu-doped TiO_2 for the effective reduction of nitro-aromatic contaminants.

Agileo Hernández-Gordillo[1,2], Vicente Rodríguez González[1*]

[1] División de Materiales Avanzados, Instituto Potosino de Investigación Científica y Tecnológica, Camino a la Presa San José 2055 Col. Lomas 4a. sección C.P. 78216, San Luis Potosí, S.L.P., México.

[2] CIIEMAD, Instituto Politécnico Nacional, Calle 30 de Junio de 1520 s/n, Barrio la Laguna Ticomán C.P. 07340, Del. Gustavo A. Madero México, D.F. Tel. 57 29 60 00.

The addition of Cu species via copper glycine complexes as a strategy for doping the TiO_2 structure during the sol-gel process produces a copper-TiO_2-based composite. The combination of the copper-TiO_2-based composite with the practical UV functionalization of highly dispersed silver nanoparticles (AgNPs), 3 nm, results in an efficient photocatalyst for eliminating 4-nitrophenol as a model of nitro-aromatic contaminant. This novel Ag/TiO_2-Cu composite achieved the effective photoreduction of 4-nitrophenol into the valuable 4-aminophenol in approximately 30 min with high conversion (96 %). A possible reduction mechanism of aromatic nitro compounds into amines in aqueous alkaline medium is discussed, considering the interfacial fast charge transfer during the *in situ* reduction of copper by the presence of hydrazine as a sacrificial electron donor.

Keywords: Hydrazine reagent, 4-nitrophenol reduction, Cu-doped TiO_2, AgNPs photoactivity, copper glycine complexes.

1. Introduction

Noble metals such as gold, silver, and platinum, among others, have been used to enhance the photoactive properties of titanium dioxide [1]. The studies have been focused principally on the photo-oxidation of organic contaminants such as dyes, phenols or pesticides [1-2]. The strategy is to use metallic nanoparticles (MNPs), either doped in frameworks or loaded on surfaces, as electron captors, metallic scavengers or interfacial charge transfer agents. Novel properties of the metallized TiO_2 have been discussed in photocatalytic applications such as Surface Plasmon Resonance (SPR) states, visible-light-driven photoactivity, oxygen vacancies, and life-time of e^--h^+ pairs, although this topic is still under discussion due to the dependence of the TiO_2 crystalline phase, the size and shape of the MNPs and the ion-size effect on the TiO_2 framework [1, 3]. Photocatalysis focuses not only on the oxidation of emerging contaminants but also on the photoreduction reactions that generate sustainable sources of energy such as hydrogen production, and the reduction of nitro-aromatic contaminants, and the ways to control the photo-inactivation of pathogenic microorganisms [4-6]. A representative hazardous and endocrine disruptor of nitro-aromatic chemicals is 4-nitrophenol (*4-NP*). *4-NP* is used commonly for the manufacture of drugs, fungicides, insecticides, dyes and to darken leather. Serious inhalation or ingestion of *4-NP* by human beings cause headaches, drowsiness, nausea, and cyanosis, and the immediate contact with the eyes causes irritation [7]. Chemical and photoassisted reductions have been explored in recent times to achieve the reduction of nitro-aromatic compounds into harmless or valuable amino reagents by using TiO_2, CdS, and graphene hybrids, among other catalysts [8-11]. The photocatalytic reduction of *4-NP* has been reported as a promising practical way to yield valuable amino reagents for chemical products [11-12].

In this work, the effect of incorporating copper nanoparticles via the copper-diglycinate complex into the TiO_2 framework during a sol-gel process is studied; in addition, the UV functionalization of AgNPs on the surface of Cu-doped TiO_2 was carried out in order to have MNPs as co-catalysts. The kinetics of the selective reduction of *4-NP* to 4-aminophenol (*4-AP*) over the Ag/TiO_2-Cu photocatalysts is studied in correlation with the physicochemical characterization of the Ag/TiO_2-Cu photocatalysts. A possible reduction mechanism is also suggested.

2. Experimental

2.1 TiO_2–Cu Synthesis

Copper doped TiO_2 was prepared by a sol–gel procedure, via the incorporation of copper glycine complexes [13]. Firstly, the copper-diglycinate complex was prepared using $Cu(NO_3)_2.3H_20$ (Aldrich, 98%) and glycine (Sigma-Aldrich, 99%) as precursors in hot distilled water. The doped semiconductors were prepared, based on the alkoxide/ethanol/water molar ratio of 1/3/8, as follows: the appropriate complex solution and titanium (IV) isopropoxide (Aldrich, 97%) were simultaneously added dropwise to a solution containing ethanol-deionized water at 70°C. Then, the solution was maintained under vigorous stirring for 2 h and under reflux for 48 h to obtain a colloidal solution that was dried in air at 70 °C for 12 h. Finally, the obtained powders were annealed in air at either 400 or 600°C for 4 h. The copper amount was calculated to obtain 1 wt% Cu. Undoped titania was prepared under the very same conditions used for the TiO_2–Cu samples. The undoped titania sample was labeled as T–SG, where SG stands for sol–gel, while the Cu-doped titania samples were labeled as T–Cu.

2.2 Photoreduction of silver nanoparticles over the TiO_2-Cu substrate.

The photoreduction of silver nanoparticles was carried out over the sol-gel T-Cu and commercial P25 provided by Evonik Degussa GmbH [6-14]. The appropriate TiO_2-Cu powder was added to 50 mL of alcoholic solution of $AgNO_3$, and the slurry was maintained for 30 min under continuous magnetic stirring to achieve the adsorption equilibrium of the Ag^+ ions on the TiO_2-Cu surface. Afterwards, the slurry was irradiated at room temperature with a commercial germicidal lamp (TecnoLite G15T8, 214 nm, 17 W) for 60 min under vigorous stirring. The fresh preparation was dried overnight in an oven at 100 °C. The silver nanocomposites were labeled as Ag/T-Cu; bare Ag/T-SG and Ag/P25 samples were also prepared under identical conditions. The silver amount was calculated to obtain 2 wt% Ag.

2.3 Characterization of Ag/T–Cu and bare photocatalysts.

Powder X-ray diffraction (XRD) measurements (Brucker D8 Advanced diffractometer, Cu Kα radiation, from 10 to 80°) were used to identify the crystalline phases of the copper doped TiO_2 semiconductors. The particle sizes were calculated from the peak widths using the Scherrer equation: $D = k\ 0.89/b\ cos\ h$, where D is the average particle size, k is the X-ray wavelength (1.5404 Å) and b is the half-width of the (101) anatase peak at 25.2° of 2 theta (h). UV–Vis diffuse reflectance spectroscopy was performed by means of an Agilent Technologies Series 5000 spectrometer with an integration sphere. The samples were placed in a Teflon cell to measure the reflectance reemission function. Band-gap energies were estimated by a straight line extrapolated from the F(R) curve to the abscissa axis in eV. When the abscissa has a value of zero, then Eg = hν. The morphology and semiquantitative composition of the photocatalyst was revealed by field emission scanning electron microscopy (FESEM) using a Helios NanoLab 600i equipped with Advanced Dual Beam coupled with an EDX detector. STEM-HAADF analysis, by means of transmission electron microscopy (TEM) performed on a Tecnai FEI 300 microscope operated at 300 kV, was carried out in order to identify the AgNPs. The specific surface areas were measured

by the BET method. Prior to N_2 admission into the cell, all the semiconductors were degassed at 200 ◦C for 12 h under vacuum.

2.4 Photoreduction of 4-nitrophenolate (*4-NPate*)

The photoreduction reaction of *4-NPate* was performed in a glass home-made reactor system containing 200 mL of aqueous solution with 8.5 ppm of *4-NP* (Aldrich), 0.5 M of N_2H_4 (Aldrich) and 0.05-0.2 g/L of the photocatalyst powder. The suspension was maintained under magnetic stirring (600 rpm) at room temperature and was left under dark conditions for 1h to ensure the adsorption-desorption equilibrium. Afterwards, the suspension was irradiated with UV light supplied by a high pressure Hg lamp emitting λ=254 nm, of 4400 μW/cm^2 encapsulated into a concentric quartz tube immersed into the slurry. The estimation of the *4-NP* concentration was made by UV-Vis spectroscopy using a Varian-Cary 5000 spectrometer, following the disappearance of the absorption band at 400 nm for *4-NPate*. The Langmuir-Hinshelwood kinetic model is usually applicable to describe the kinetics of *4-NP* reduction. So, kinetic data such as the apparent rate constant (k_{app}) for reduction reactions were obtained considering a pseudo zero order process [15].

3. Results and discussion

In Figure 1, selected diffraction patterns of both T-Cu sol-gel samples annealed at 400 and 600°C with functionalized AgNPs are shown. The main diffraction peaks observed in the patterns correspond to the TiO_2 anatase crystalline phase (JCPDS 21-1272). Neither diffraction peaks corresponding to metallic copper nor to silver particles are present; in addition, the corresponding oxide compounds (Cu_xO_y or Ag_xO_y) are not observed either. It seems that copper and silver nanoparticles are highly dispersed, copper into the superficial anatase framework and silver over the

TiO_2-Cu surface. However, the XRD technique does not detect normally metallic concentrations under 5 wt%. Low silver and copper concentrations were used in order to preserve the anatase phase and only help in the interfacial charge transfer as an electron captor during the photocatalytic process. These preparation techniques have been well established in our group as it has been shown in previous works [13]. In the sample stabilized at 400°C, a small diffraction peak corresponding to the TiO_2 brookite phase (JCPDS 76-1934) is observed, while when the sample was stabilized at 600°C, the crystalline TiO_2 rutile phase started to grow (JCPDS 21-1276). The anatase crystallite size determination by the Scherrer method reveals a crystallite size of 14 nm in the composite annealed at 400°C, while for the composite annealed at 600°C, the average crystallite size is almost three times bigger, 46 nm. According to literature results [16], after annealing Ag,Cu/TiO_2-P25 nanoparticles at 650°C, the main obtained TiO_2 crystalline phase was rutile with a crystallite size of 27 nm. In our sol-gel process with copper-diglycinate complex as copper precursor, the titania preserves practically the 96.0% of the anatase phase after annealing for 4h at 600°C (See Supplementary material), which suggests that doping TiO_2 with Cu^{2+} ions may delay the crystal growth process and probably most of the copper incorporation takes place on the surfaces of the crystallites; by increasing the annealing temperature to 600°C, the Cu^{2+} ions are segregated out of the surface and grow probably as copper oxide. The homogeneous green light color of the samples indicates the presence of copper in TiO_2. The ICP-OES analysis of the T-Cu 400°C sample gives 0.651 wt% of copper, which is lower than the theoretical composition, thus confirming the presence of copper in the TiO_2 framework. The aim of using a glycine copper complex was to obtain, eventually, a co-doped material with nitrogen or carbon; however, the ICP-OES analysis did not detect nitrogen or carbon content in the final sample. The glycine complex allowed the doping of the TiO_2 framework, then a complete evacuation of the complex organic part was achieved by annealing the sample at 400 or 600°C.

The SEM image shows the typical morphology of TiO_2 nanoparticles with irregular shape and agglomerated to form larger particles, Fig 2a. In addition, functionalized silver nanoparticles were observed on the surface of the TiO_2 crystallite. These silver particles are homogeneously distributed over the surface of the crystallites, with no preferential sites. The EDX analyses enabled us to confirm that silver and copper nanoparticles are present in the TiO_2 composites, Ag/T-Cu, Fig. 2b.

The STEM-HAADF (High Angle Annular Dark Field) image of Ag/T-Cu 400 confirms the presence of AgNPs highly monodispersed over the T-Cu surface with an average size of 3 nm, Fig 2c. The size of the T-Cu 400 particles is 13 nm, which is in good agreement with the XRD crystallite size results.

The reflectance diffuse characterization shows the selected UV-Vis spectra of the materials with and without the incorporation of silver nanoparticles, Fig 3a. A slight shift to the visible region was observed in the AgNPs functionalized over the T-Cu substrate annealed at 600°C; furthermore, a Surface Plasmon Resonance (SPR) band is observed at around 2.65 eV for Ag/T-Cu 600 and 2.40 eV for Ag/T 600. These resonance absorbances were attributed to AgNPs around 3 nm over the TiO_2 surface [6]. Copper incorporation seems to have a dispersion effect on the AgNPs in TiO_2, since the Ag/T-Cu 400 photocatalyst does not show a SPR band, while AgNPs deposited onto the TiO_2 support reveals the most intense SPR band. The band-gap energies range from 3.14 to 3.25 eV. The sol-gel preparation gives a homogenous anatase crystalline phase with copper ions dispersed into the framework. The copper complex helps to control hydrolysis during the sol-gel process and allows the copper incorporation into the framework because the effective ionic radii of Cu^{2+} is smaller than those featured by O^{2-} and Ti^{4+}. Silver functionalization also probably helps the slight red-shift of the band-gap energies. The band-gap energies of the loaded sol-gel semiconductors allow the photoexcitation in UV light, and the copper ions in the framework can be able to minimize the charge recombination and the AgNPs cap the electrons to be transferred to the nitro-aromatic contaminant.

The N_2 adsorption-desorption isotherms and pore size distributions are presented in Fig. 3b. According to the IUPAC, the isotherms are Type IV, characteristic of TiO_2 mesoporous materials; however, the absorbed volume decreased as the annealed treatment was increased. The specific surface area of the Ag/T-Cu 400 sample decreased from 97.83 to 31.44m^2/g when it was annealed at 600 °C (Ag/T-Cu 600). In addition, the pores size distribution (inset in Fig. 3b)) exhibited a different behavior, where the average pore size is about 10 nm for the Ag/T-Cu 400 sample and 17 nm with low pore volume in the case of the crystalline Ag/T-Cu 600.

3.1 Photocatalytic activity

The aqueous solution of 4-nitrophenol *(4-NP)* shows the characteristic absorption band at 400 nm of the 4-nitrophenolate *(4-Npate)* ion species in alkaline media by the presence of hydrazine [15]. No adsorption of *4-NPate* on the surface of the photocatalysts was observed for 1 h of adsorption–desorption equilibration under dark conditions when the photocatalyst was added. Under this dark condition, only for the T-Cu 400 photocatalyst, the characteristic light green color of the photocatalyst immediately turned to dark gray, which was observed from the reactor glass window when the powdered photocatalyst came in contact with hydrazine into the aqueous *4-NP* solution. This color change can be associated with the *in situ* copper reduction at room temperature by the presence of hydrazine [17, 18]. After the UV irradiation process, when the Ag/T-Cu 400 composite was used, the absorption band of the *4-NPate* ion got reduced within 25 min of irradiation and a new absorption band at 295 nm, characteristic of the 4-aminophenol (*4-AP*) formation was built-up (Figure 4) [19, 20]. The presence of two isosbestic points at 280 and 313 nm indicates equilibrium between the two components (*4-NPate* and *4-AP*) without any secondary product formation [19].

The plot C/C_0 versus time for the photoreduction of *4-NPate* (Figure 5) exhibits a good linear correlation with 70% of conversion for the three used photocatalysts (T-SG, T-Cu 400 and Ag/T-Cu 400), which suggests that the photoreduction rate is independent of the decreasing *4-NPate*

concentration, which is characteristic of the zero order rate kinetics [15, 11]. High conversion (96 %) from *4-NPate* to *4-AP* was achieved with the Ag/T–Cu 400 composite at ~30 min and when T–Cu 400 without AgNPs was used, at 1.1 h of the reaction, the conversion was 91 %.

The apparent zero order rate constant value of the photoreduction of *4-NPate* in the absence of any photocatalyst (photolysis) is very low (k=0.04 Mh^{-1}), and when the T–Cu 400 photocatalyst was added, the rate constant value was linearly increased as the photocatalyst load was increased too (Figure 6), obtaining a rate constant value of 1.15 Mh^{-1} with 0.15 g/L of photocatalyst load. But this rate constant value decreased at photocatalyst loads up to 0.15 g/L because of the light scattering phenomena, which implies an increase in the optical density of the total suspension at the wavelength of the exciting light (254 nm) [22].

The photoreduction rate of the *4-NPate* ion with the bare T-SG photocatalyst is low (0.74 $Mh^{-1,}$ Figure 7), but when TiO_2 was doped with Cu (T-Cu 400), the photocatalytic reduction rate was improved 1.55 times (1.15 Mh^{-1}). A similar rate constant value was obtained when P25 was used as reference photocatalyst (1.17 Mh^{-1}); however, when AgNPs were deposited on T–Cu 400, the photocatalytic reduction rate was higher (2.4 Mh^{-1}) than that of the Ag/P25 photocatalyst (1.78 Mh^{-1}), suggesting that the presence of silver nanoparticles in T-Cu 400 improved two times the electron transfer process [23]. The photocatalytic activities of Ag/T 400 and Ag/T 600 were improved in the same order (not shown) with similar rate constant values. In addition, the photoreduction rate of *4-NPate* using the Ag/T–Cu 600 composite (annealed at 600°C) is apparently similar to that of the composite annealed at 400°C, however, considering that the specific surface area of Ag/T–Cu 400 is higher than that of Ag/T–Cu 600, the intrinsic kinetic value for the last sample resulted to be the highest (2.44 $Mh^{-1}m^{-2}$). The intrinsic kinetic value for the sample annealed at 400 °C was close to that of the Ag-TiO_2-P25 reference (0.85 $Mh^{-1}m^{-2}$). The results suggest that the electron transfer process is improved by the crystal growth of the anatase phase.

3.2 Mechanism of nitro-aromatic reduction

The photocatalytic reduction of *4-NP* using the bare TiO_2-SG semiconductor in the presence of hydrazine follows a similar mechanism previously reported [15], where the photogenerated h^+ reacts with hydrazine to form the hydrazyl radical (NH_2NH^*), while the photogenerated e^- are transferred from the TiO_2 surface to the acceptor nitro-aromatic contaminant via the electron transfer process. On the other hand, when the well crystallized TiO_2 anatase is doped with copper oxide (Cu_2O), the photoreduction rate of *4-NP* is improved, but the fast electron transfer follows a different mechanism path. In this case, considering that during the adsorption-desorption process of the *4-NPate* suspension with the T-Cu 600 photocatalyst, Cu^+ was reduced to Cu^0 by the presence of hydrazine due to its strong reducing properties (-1.15 eV), [24] and the reduction potential of the Cu^+/Cu^0 couple is 0.52 eV [25], therefore, the *in situ* copper reduction is feasible [18] at room temperature under dark conditions. Thus, during the irradiation process, the reduced Cu^0 embedded in TiO_2 anatase (Figure 8-A) improved the electron transfer process due not only to the high crystallization of the anatase phase but also to the work function of copper (4.5-4.7 eV) [26, 27]. Because of the band-gap excitation state, the photogenerated e^- flow to the metal nanoparticles, whereas the h^+ move to the semiconductor, yielding an efficient separation of the charge carriers as well [28], and as a consequence, achieving a fast *4-NPat*e photoreduction rate. In addition, the presence of AgNPs on the T-Cu 600 surface increases the efficiency of the interfacial charge transfer (Figure 8-B); on the one hand, due to the similar work function of silver (4.7 eV) to that of copper [28], and on the other hand, due to the ability of the Ag nanoparticles to oxidize hydrazine [15, 29], allowing the fast electronic transfers.

Conclusion

In conclusion, this work reports the sol-gel synthesis of Cu-doped TiO_2 using a Cu-diglycinate complex followed by the practical UV functionalization with highly monodispersed AgNPs (3 nm).

Hydrazine, as a sacrificial electron donor into an aqueous 4-nitropehnol solution, led to the *in situ* reduction of copper on the Cu-doped TiO_2, achieving a high photocatalytic reduction rate of 4-nitrophenol under UV light irradiation. The presence of AgNPs on the doped TiO_2-Cu^0 led to a fast charge transfer process, achieving the formation of valuable aminophenol in 30 min with high conversion (96%).

Acknowledgements

The authors gratefully acknowledge G. Labrada Delgado and B. Rivera Escoto from LINAN-IPICYT, for the SEM and XRD characterizations of the materials studied in this work. We also thank Hugo Ivan Mendoza Leos for his valuable technical assistance in the experimental synthesis during the program "Verano de la Ciencia región centro, 2013-Academia Mexicana de las Ciencias". We thank CONACYT for the financial support provided through the SEP CONACYT-CB-2011/169597 project.

Available supplementary material: [Average particle size determination from STEM-HAADF analysis, Rutile and brookite phase quantifications].

References

[1]. S. G. Kumar, L. G. Devi, Review on Modified TiO_2 Photocatalysis under UV/Visible Light: Selected Results and Related Mechanisms on Interfacial Charge Carrier Transfer Dynamics J Phys. Chem. A 115 (2011) 13211-13241

[2]. M. Maicu, M.C. Hidalgo, G. Colón, J.A. Navío, Comparative study of the photodeposition of Pt, Au and Pd on pre-sulphated TiO_2 for the photocatalytic decomposition of phenol, J. Photochem. Photobiol. A: Chem 217 (2011) 275-283

[3]. J. Choi, H. Park, M. R. Hoffmann, Effects of Single Metal-Ion Doping on the Visible-Light Photoreactivity of TiO_2, J. Phys. Chem. C, 114 (2010) 783–792

[4]. G. Li-Puma, V. Rodríguez-González, A. Pérez-Larios, Photocatalysis from the treatment of emerging contaminants to energy, J Hazard Mater 263 (2013) 1

[5]. J. G. Yu, Y. Hai, B Cheng, Enhanced Photocatalytic H-Production Activity of TiO_2 by $Ni(OH)_2$ Cluster Modification, J. Phys. Chem. C 115 (2011) 4953-4958

[6]. S-W. Lee, L.M. Lozano-Sánchez, V. Rodríguez-González, J. Hazard. Mater. 263 (2013) 20-27

[7] http://www.epa.gov/ttn/atw/hlthef/nitrophe.html

[8]. S. Saha, A. Pal. S. Kundu, S. Basu, T. Pal, Photochemical green synthesis of calcium-alginate-stabilized Ag and Au nanoparticles and their catalytic application to 4-nitrophenol reduction, Langmuir 26 (2010) 2885-2893

[9]. X. Chao, Y. Yao, Y. Rusheng, F. Xianzhi, Enhanced photocatalytic performances of TiO_2-graphene hybrids on nitro-aromatics reduction to amino-aromatics, RSC Advances 3 (2013) 18002-18008

[10]. A. Shivhare, S. J. Ambrose, H. Zhang, R. W. Purves, R. W. J. Scott, Stable and recyclable Au_{25} clusters for the reduction of 4-nitrophenol, Chem. Commun. 49 (2013) 276

[11]. A. Hernández-Gordillo, A. G. Romero, F. Tzompantzi, R. Gómez, Kinetic study of the 4-Nitrophenol photooxidation and photoreduction reactions using CdS, Appl. Catal. B: Environ. 144 (2014) 507-513

[12]. S. Sarkar, A. K. Guria, N. Pradhan, Influence of doping on semiconductor nanocrystals mediated charge transfer and photocatalytic organic reaction, Chem. Commun. 49 (2013) 6018-6020.

[13]. V. Rodríguez-González, E. Marceau, M. Che, C. J. Pepe, Solid State Chem. 180 (2007) 3469–3478

[14]. S. Obregon-Alfaro, V. Rodriguez-Gonzalez, A. A. Zaldivar-Cadena, S. W. Lee, Sonochemical deposition of silver–TiO_2 nanocomposites onto foamed waste-glass: Evaluation of Eosin Y decomposition under sunlight irradiation. Catal. Today 166 (2011) 166

[15]. A. Hernández-Gordillo, M. Arroyo, R. Zanella, V. Rodríguez-González, Photoconversion of 4-Nitrophenol in the presence of Hydrazine with AgNPs-TiO_2, J. Hazard. Mater. 268 (2014) 84-91.

[16]. M. A. Behnajady, H. Eskandarloo, Silver and copper co-impregnated onto TiO_2-P25 nanoparticles and its photocatalytic activity, Chem. Eng. J. 228 (2013) 1207–1213.

[17]. Y. Li, W-N Wang, Z. Zhan, M-H Woo, C-Y Wu, P. Biswas, Photocatalytic reduction of CO_2 with H_2O on mesoporous silica supported Cu/TiO_2 catalysts, Appl. Catal. B: Environ. 100 (2010) 386–392.

[18]. K. S. Tan, K. Y. Cheong, Advances of Ag, Cu, and Ag–Cu alloy nanoparticles synthesized via chemical reduction route, J. Nanopart. Res. 15 (2013) 1500-1537.

[19]. S. Wunder, F. Polzer, Y. Lu, Y. Mei, M. Ballauff, Kinetic Analysis of Catalytic Reduction of 4-Nitrophenol by Metallic Nanoparticles Immobilized in Spherical Polyelectrolyte Brushes, J. Phys. Chem. C 2010, 114, 8814–8820.

[20].S. Gu, W. Wang, F. Tan, J. Gu, X. Qiao, J. Chen, Facile route to hierarchical silver microstructures with high catalytic activity for the reduction of p-nitrophenol, Mater. Res. Bull. 49 (2014) 138–143.

[21]. P. Yang, A-D Xu, J. Xia, Jie He, H-L Xing, X-M Zhang, S-Y Wei, N-N Wang, Facile synthesis of highly catalytic activity Ni–Co–Pd–P composite for reduction of the p-Nitrophenol, Appl. Catal. A: General 470 (2014) 89– 96.

[22]. B. Pullman, N. Golgdblum, Excited states in organic chemistry and biochemistry, Reidel Publishing Company, Dordreeht Holland (1997) 40-42.

[23]. M. M. Mohamed, M. S. Al-Sharif, One pot synthesis of silver nanoparticles supported on TiO_2 using hybrid polymers as template and its efficient catalysis for the reduction of 4-nitrophenol, Mater. Chem. Phys. 136 (2012) 528-537.

[24]. M. G. Macnaughton, G. A. Urda, S. E. Bowden, Oxidation of hydrazine in aqueous solution, INTERIM REPORT, Civil and Environmental Engineering Development office, Florida (1978).

[25]. V Jeyalakshmi, R Mahalakshmy, K R Krishnamurthy & B Viswanathan, Titania based catalysts for photoreduction of carbon dioxide: Role of modifiers, Indian J. Chem. 51A (2012), 1263-1283.

[26]. P. A. Anderson, The Work Function of Copper, Phys. Rev. 76 (1949) 388-390.

[27]. Y. Shiraishi, H. Sakamoto, Y. Sugano, S. Ichikawa, T. Hirai, Pt-Cu Bimetallic Alloy Nanoparticles Supported on Anatase TiO_2: Highly Active Catalysts for Aerobic Oxidation Driven by Visible Light, ACS nano 7 (2013) 9287–9297.

[28]. X. Zhang, Y. L- Chen, R-S Liu, D. P. Tsai, Plasmonic photocatalysis, Rep. Prog. Phys. 76 (2013) 046401 (41pp).

[29]. G-W Yang, G-Y Gao, C. Wang, C.-L Xu, H-L Li, Controllable deposition of Ag nanoparticles on carbon nanotubes as a catalyst for hydrazine oxidation, Carbon 46 (2008) 747–752.

Figure Captions

Figure 1. XRD patterns of the photocatalysts treated thermally at either 400 or 600°C. All the observed crystalline TiO_2 phases are indexed in the figure.

Figure 2a. SEM image for the Ag/T-Cu 400 composite.

Figure 2b. EDX spectra for the Ag/T-Cu 400 composite.

Figure 2c. STEM-HAADF image of Ag/T-Cu 400, which confirms the presence of AgNPs on the T-Cu surface.

Figure 3a. F(R) as a function of the spectrum wavelength of functionalized silver and unfunctionalized photocatalyst.

Figure 3b. N_2 adsorption-desorption isotherms of Ag/T-Cu 400 and Ag/T-Cu 600 (pore size distribution is the inset).

Figure 4. UV-Vis spectra for the photoreduction of *4-NPate* in the presence of hydrazine with Ag/T–Cu 400 composite.

Figure 5. C/C_0 versus time plot for the photoreduction of 4-NPate with: a) T-SG, b) T–Cu 400 and c) Ag/T–Cu 400 composites.

Figure 6. Apparent zero order rate constant of the photoreduction of *4-NPate* with T–Cu 400 photocatalyst as a function of the photocatalyst load.

Figure 7. Comparison of the photoreduction rate of *4-NPate* for all the evaluated photocatalysts.

Figure 8. Schematic representation of the mechanism of the nitroaromatic photoreduction in the presence of hydrazine with: a) doped TiO_2-Cu, and b) Ag/TiO_2-Cu composite.

Figure 1.

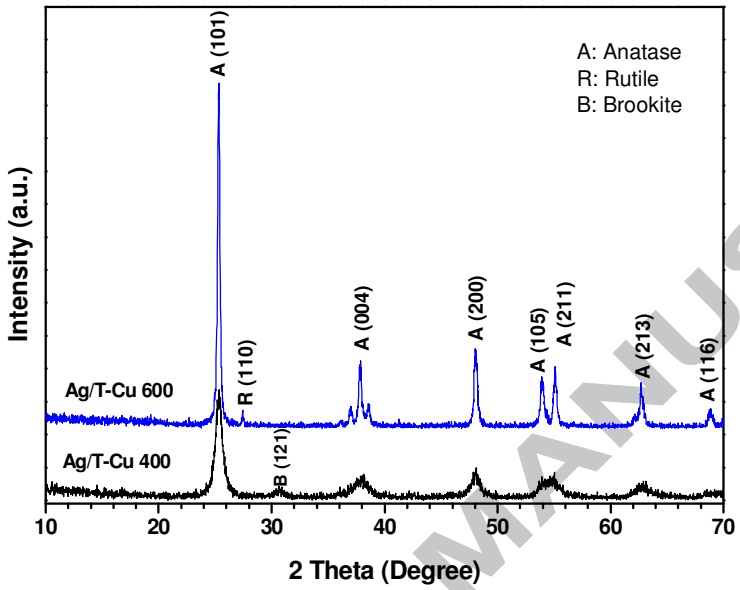

Figure 2a)

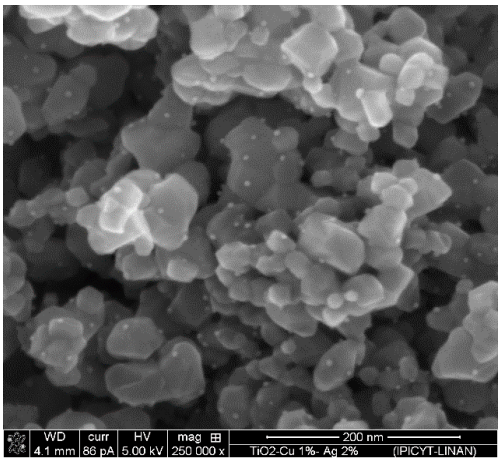

Figure 2b)

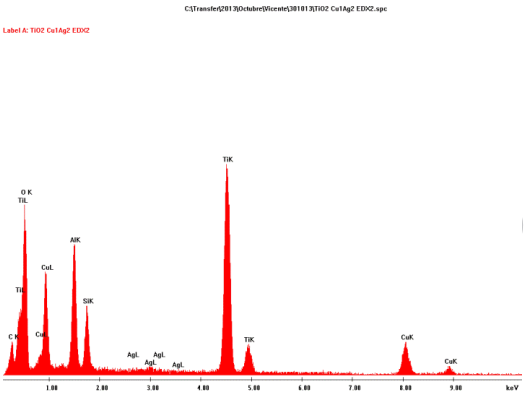

Figure 2c)

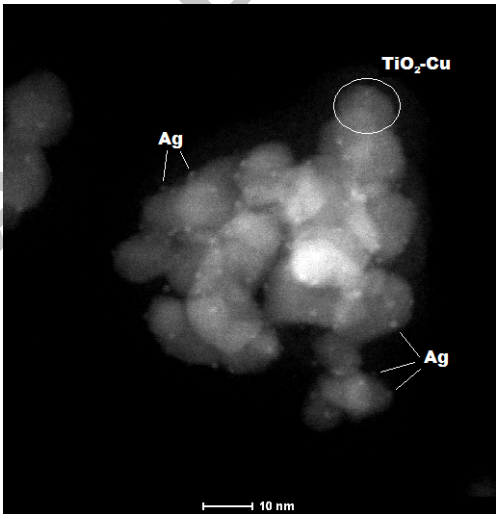

Fig. 3a

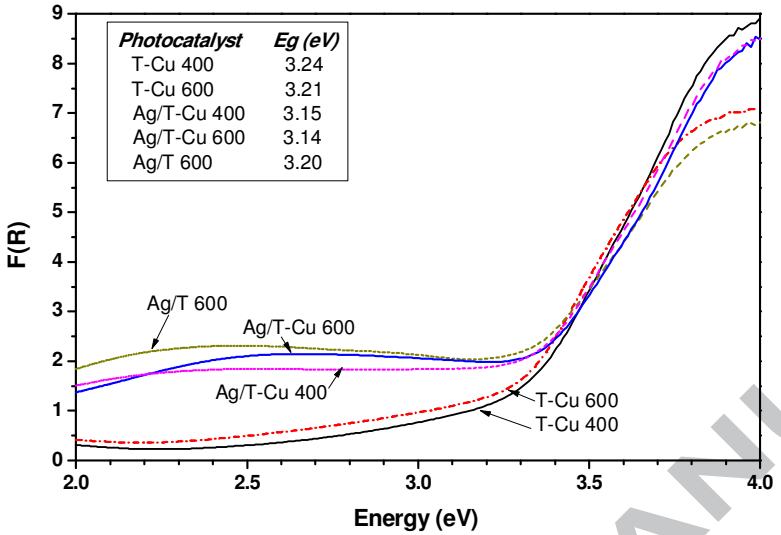

Fig. 3b

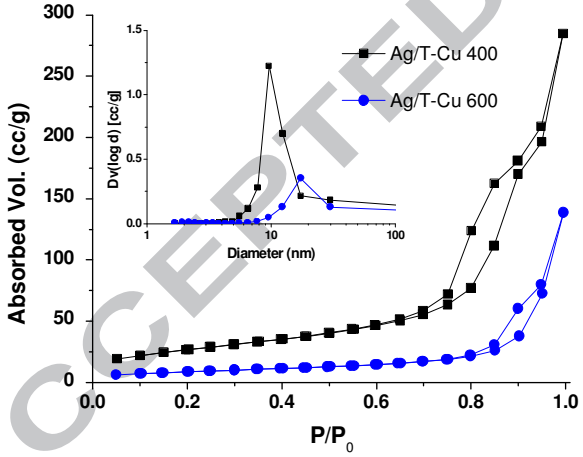

Figure 4.

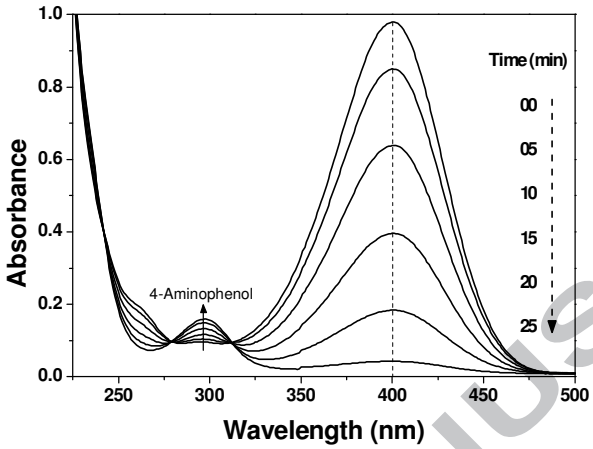

Figure 5.

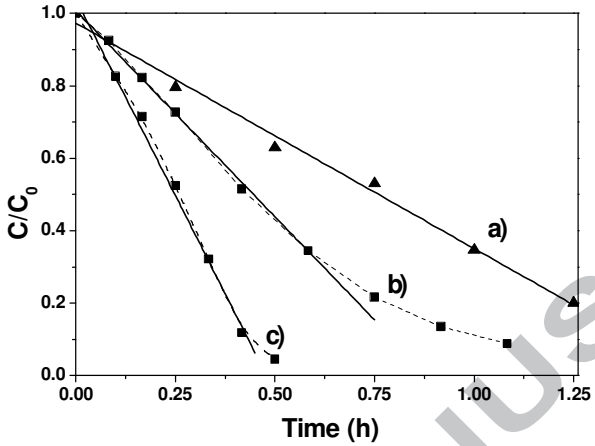

Figure 6.

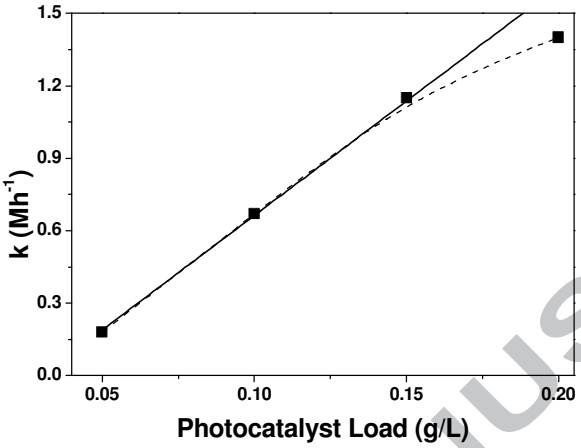

Figure 7.

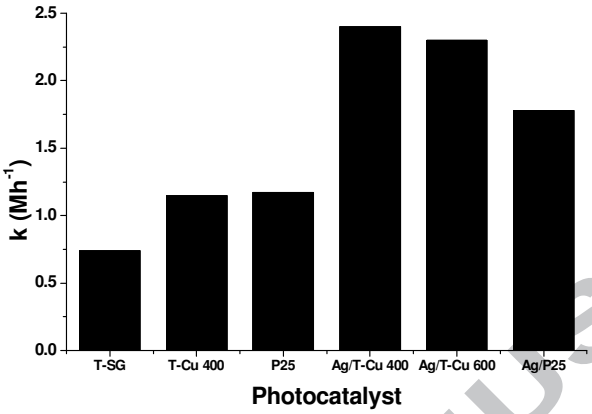

Figure 8.

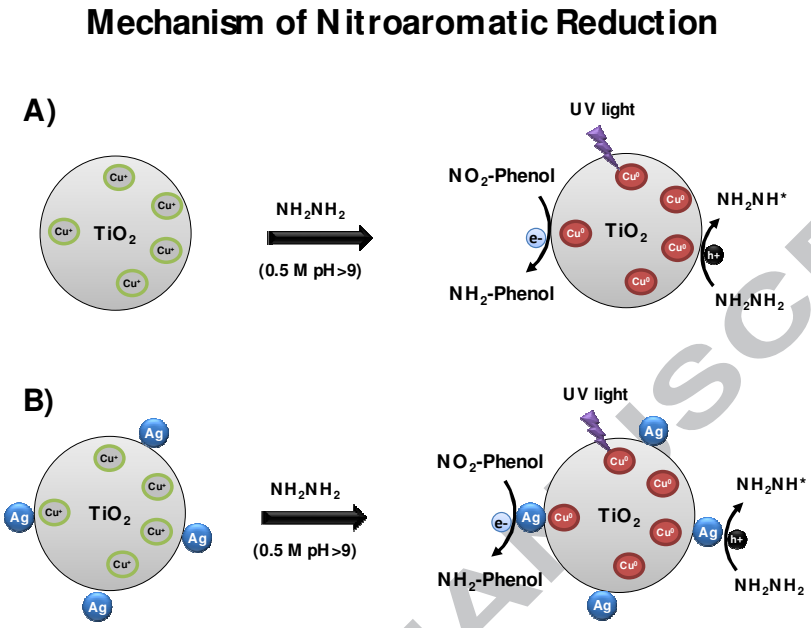

Highlights

The use of a Cu-diglycinate complex as dopant produces homogeneous Cu-doped TiO_2.

AgNPs functionalized over Cu-doped TiO_2 enhance the interfacial charge transfer.

Hydrazine as a sacrificial electron donor led to the *in situ* copper reduction.

Effective *4-NPate* photoreduction was achieved in 30 min with high conversion.